JOURNAL OF CATALYSIS 141, 337–346 (1993)

Neopentane Conversion Catalyzed by Pd in L Zeolite: Effects of Protons, Ions, and Zeolite Structure

Z. KARPIŃSKI,[1] S. N. GANDHI, AND W. M. H. SACHTLER

V. N. Ipatieff Laboratory, Center for Catalysis and Surface Science, Northwestern University, Evanston, Illinois 60208

Received September 1, 1992; revised December 15, 1992

The conversion of 2,2-dimethylpropane (neopentane) has been studied over zeolite-L-supported Pd catalysts; the results are compared with data for Pd on zeolite Y. Variation of the charge compensating ion (Li^+, K^+, or Ca^{2+}) in L has only a moderate effect on the catalytic parameters, due either to variations in the heat of physisorption or to "electronic" effects on Pd. The reduction temperature, T_R, of Pd/L samples that have previously been calcined at 250°C, strongly affects the catalytic performance: after T_R = 250°C, sufficient NH_3 ligands of the ion exchanged $Pd(NH_3)_4^{2+}$ ions survive to neutralize the protons that are formed during reduction; catalytic activity then increases during reaction while NH_4^+ ions decompose and Pd-proton adducts of high catalytic activity are formed. At T_R = 400°C, the NH_3 ligands are destroyed and this catalyst is stable and very active. Activity, selectivity, and kinetic parameters depend on the structure of the support; apparent activation energies, E_a, are in the range of 45–55 kcal/mol for Pd/Y, but 75–90 kcal/mol for Pd/L. A linear relation between E_a and log of the preexponential factor is obtained. While classical pore-diffusion operates in Y, *single-file* diffusion appears more likely in L; i.e., channels tend to be plugged with physisorbed molecules at low temperature. The difficult of primary reaction products to escape from the pores correlates with a higher fraction of secondary products observed for Pd/L vis-à-vis Pd/SiO_2. It is conceivable that different diffusion types also contribute to the different E_a values for zeolites with three-dimensional or unidimensional channel systems.

I. INTRODUCTION

In pioneering research, Dalla Betta and Boudart (*1*) and Foger and Anderson (*2*) found that zeolite-Y-supported platinum is much more active in catalyzing the conversion of neopentane than Pt is on amorphous supports such as Al_2O_3 or SiO_2. The authors attributed this enhanced activity to electron-deficient platinum. XPS results indicated that the electron-deficiency depends on the nature of the charge-compensating cation in the zeolite (La^{3+}, Ca^{2+}, Na^+). The present authors observed an enhanced activity for zeolite-supported palladium; the activity was found to be dependent on the proton concentration (*3–5*). On Pd/NaY containing two protons per reduced Pd atom, the turnover frequency for neopentane conversion was roughly two orders of magnitude higher than that on Pd/SiO_2. This result was ascribed to the formation of $[Pd_n\text{-}H_x]^{x+}$ adducts; i.e., electron-deficiency of Pd is ascribed to electron sharing with zeolite protons. The model was verified by Stakheev and Sachtler (*6*), who showed by XPS that Pd in NaHY carries a partial positive charge. The extent of the electron-deficiency depends on the proton concentration and the size of the Pd clusters, in agreement with the model of $[Pd_n\text{-}H_x]^{x+}$ adducts. Electron-rich platinum particles have also been reported, e.g., in KL, in the absence of a high proton concentration (*7*).

While $[Pd_n\text{-}H_x]^{x+}$ adducts display an enhanced catalytic activity for neopentane

[1] On leave from Institute of Physical Chemistry, Polish Academy of Sciences, Warszawa, Poland.

0021-9517/93 $5.00

conversion and also carry a positive charge, it is uncertain whether electron-deficiency is the actual cause of the modified catalytic activity. It is also conceivable that the H atoms in the $[Pd_n\text{-}H_x]^{x+}$ adducts are chemically involved in the catalysis of neopentane conversion or that the peculiar transport phenomena inside zeolite channels affect turnover frequencies and slopes of Arrhenius curves.

In addition to the electronic nature of supported Pd or Pt particles, the zeolite structure may also have a significant effect on catalytic activity. Zeolites of faujasite structure have three-dimensional pores providing numerous paths between each site and the gas phase outside the zeolite. Supercages can act as "mixing chambers" for reactants and products. A different situation is encountered with zeolites with one-dimensional narrow pores under conditions where physical adsorption of reactants is appreciable. Two-way traffic of reactant and product molecules is virtually impossible inside pores too narrow for molecules to pass each other. In the terminology of Rieckert (*8*) and Kärger *et al.* (*9*), ordinary diffusion is replaced by "single-file" diffusion, i.e., molecules move like pearls on a string. Catalytic conversions near the pore mouths are registered in the gas phase, but regions far from pore orifices are virtually isolated from the gas when the density of physisorbed molecules inside the channels is high. The region which effectively communicates with the gas phase increases with temperature, thus the apparent activation energy is affected.

In the present work neopentane conversion is studied over Pd/XL with X = K^+, Li^+, Ca^{2+}, NH_4^+, and H^+ as charge-compensating ions, because it has been proposed that these ions affect the electronic structure of the metal (*7, 10*). Pd is introduced by ion exchange of $Pd(NH_3)_4^{2+}$ ions; by varying the calcination and reduction temperature the concentration of protons is varied: they are formed during the reduction of Pd ions, but are neutralized if NH_3 groups survive calcination and reduction.

II. EXPERIMENTAL

a. Catalyst Preparation

The KL support was obtained from Tosoh Corp. (HSZ-500 KOA); LiKL and CaKL were prepared by ion-exchange of KL. Fifteen g of KL was slurried in 3 liters of a 0.5 *M* solution of $LiNO_3$ or $Ca(NO_3)_2$, respectively, and stirred continuously for 24 h. After it was filtered and dried in air, the support was calcined to induce ion migration. The calcination was carried out in a flow of UHP O_2 (1000 ml/min/g) and ramping the temperature from room temperature to 200°C (0.3°C/min), then from 200°C to 400°C (0.5°C/min) and holding at 400°C for 3 h. After this calcination a second exchange was carried out, again using 0.5 *M* solutions of $LiNO_3$ and $Ca(NO_3)_2$.

Pd was introduced by ion exchange. A solution of $Pd(NH_3)_4(NO_3)_2$ was added dropwise to a continuously stirred slurry of the support in doubly deionized water (200 ml/g). The ion exchange was carried out for a period of 36 h. The slurry was filtered, washed with doubly deionized water and air dried for 24 h. Atomic absorption spectroscopy of inductively coupled plasma was used to determine the metal loading. The catalysts were found to contain 3 ± 0.3 wt% Pd.

b. Catalyst Pretreatment

Prior to use, the catalysts were calcined in a flow of UHP O_2 (1000 ml/min/g) by heating from room temperature to 250°C at 0.5°C/min and holding at 250°C for 2 h, followed by purging in UHP Ar (200 ml/min/g) for 20 min and cooling to room temperature in UHP Ar. After calcination the catalysts were reduced in a flow of UHP H_2 (200 ml/min/g) by heating from 21°C to either 250 or 400°C at 8°C/min and holding at the reduction temperature for 0.5 h.

c. Temperature Programmed Desorption (TPD)

Metal dispersion was determined by integrating the desorption profiles of preadsorbed hydrogen. TPD experiments were

carried out on all three catalysts after they were calcined up to 250°C and reduced at 300°C. After reduction the sample was cooled to −78°C. The temperature of the catalyst bed was then ramped at 8°C/min up to 500°C and the rate of hydrogen evolution was monitored by a thermal conductivity detector. Integration of the TPD profile gave the total amount of adsorbed hydrogen, from which the disperson, expressed as H/Pd ratio, was calculated. All three catalysts had a H/Pd ratio of 1 ± 0.1.

d. Kinetic Studies

The reaction of neopentane with hydrogen was carried out at atmospheric pressure in a pyrex flow reactor. The catalyst (0.4 g) was deposited in a U-tube with a fritted disc and a thermocouple well. After calcination and reduction the temperature was lowered to 220°C (the initial reaction temperature) in flowing H_2. The gas flow was then changed to neopentane premixed with H_2 (1 : 9, Mattheson) and diluted with helium (UHP, Linde) to obtain a partial pressure of neopentane of 6 Torr. The total flow rate was 76 ml/min. The reaction mixture was purified by passing it through MnO/SiO_2 and molecular sieve 5A traps before the reactor. The effluent gas was analyzed by gas chromatography (HP 5790 with FID, 50m cross-linked methyl silicone capillary column). Kinetic runs began at the lowest reaction temperature. After stable conversions were observed, the temperature was increased in 10°C increments. When the extent of conversion reached 5–10%, the temperature was lowered, again in 10°C increments, and additional data were collected. A typical kinetic run resulted in 10–12 data points.

Catalytic activities were calculated as reaction rates expressed in molecules of reacted neopentane per surface Pd atom per second (TOF), assuming 100% metal dispersion. Selectivities (product distribution) were calculated in terms of neopentane consumed in the formation of a designated product (methane, ethane, propane, *i*- and *n*-butane, *i*- and *n*-pentane). Fragmentation factors, ζ, defined as the number of fragment molecules per molecule of neopentane hydrogenolyzed (*11*), were also calculated.

e. Temperature Programmed Decomposition

Temperature programmed decomposition experiments were performed to compare the ammonium ion content of samples of Pd/KL which had been calcined to 250°C and then treated as follows:

Pd/KL (400):	Reduced up to 400°C.
Pd/KL (250):	Reduced up to 250°C.
Pd/KL (250, R):	Reduced up to 250°C and exposed to reactant mixture for 2 h at 255°C.

The labels on the left are further used to refer to these three samples.

Each sample was heated in a flow of UHP He at 8°C/min from room temperature to 525°C. During this time the reactor effluent was monitored by an on-line Dycor M 100 Quadrupole Gas Analyzer.

III. RESULTS

a. Kinetic Studies

Turnover frequencies, selectivities, fragmentation factors, ζ (which characterize the depth of hydrogenolysis), and apparent activation energies are compiled in Tables 1, 2, and 3 for Pd/LiKL, Pd/KL and Pd/CaKL samples at two reduction temperatures, 250 and 400°C. Figure 1 (a,b,c) shows the Arrhenius plots for these catalysts. In this figure, hollow symbols (squares for samples reduced at 250°C, circles for samples reduced at 400°C) represent kinetic data collected while increasing the reaction temperature and filled symbols represent points collected during the return from higher to lower reaction temperatures.

Tables 1–3 show that for a given reduction temperature all three catalysts show

TABLE 1

Neopentane Conversion over 3 wt% Pd/LiKL: Product Distributions, Reaction Rates, Fragmentation Factors, and Activation Energies

Reduction temperature (°C)	Reaction temperature (°C)	Product distribution (%)[a]						TOF[b] (1/s)	ζ[c]	E_a[d] (kcal/mol)
		Me	Et	Pr	iB	nB	iP			
250	221	—	—	—	100.0	—	—	2.679×10^{-6}	1.25	
	232	25.0	—	21.0	54.0	—	—	1.644×10^{-5}	2.28	
	231.5	31.9	—	20.1	48.0	—	—	2.026×10^{-5}	2.53	
	241	34.4	—	29.8	35.8	—	—	6.705×10^{-5}	2.66	
	241	33.5	—	30.1	32.5	3.9	—	7.490×10^{-5}	2.63	50.0 ± 1.8
	251	37.3	3.9	34.9	21.2	1.4	1.3	2.419×10^{-4}	2.86	(77.1 ± 3.8)
	250.5	39.0	4.1	35.6	20.7	0.6	—	2.500×10^{-4}	2.91	
	237	35.1	—	31.4	33.5	—	—	6.114×10^{-5}	2.70	
	244	31.3	—	23.3	45.4	—	—	1.894×10^{-5}	2.52	
400	220.5	—	—	—	100.0	—	—	6.863×10^{-6}	1.25	
	221.5	26.4	—	—	73.6	—	—	1.211×10^{-5}	2.24	
	231	23.3	—	—	76.7	—	—	5.876×10^{-5}	2.12	
	231	23.3	—	—	76.7	—	—	6.070×10^{-5}	2.12	
	238	22.3	—	2.5	74.0	—	1.2	2.108×10^{-4}	2.11	88.4 ± 2.1
	237.5	22.9	—	2.2	74.8	—	—	1.864×10^{-4}	2.12	
	244	23.5	—	3.8	71.7	0.4	0.5	5.082×10^{-4}	2.15	
	243.5	23.4	—	3.9	71.8	0.4	0.4	5.005×10^{-4}	2.15	
	234	23.1	—	1.9	75.0	—	—	1.102×10^{-4}	2.12	
	225	26.9	—	—	73.1	—	—	2.686×10^{-5}	2.26	

[a] Product distribution expressed as the carbon percentage of neopentane converted to a designated product (Me = methane, Et = ethane, Pr = propane, nB = *n*-butane, iB = isobutane, iP = isopentane).

[b] Turnover frequency.

[c] Fragmentation factor, ζ, as defined in Ref. (*10*).

[d] Activation energies calculated from points measured at increasing temperature are given in parentheses, others without parentheses.

TABLE 2

Neopentane Conversion over 3 wt% Pd/KL: Product Distributions, Reaction Rates, Fragmentation Factors, and Activation Energies

Reduction temperature (°C)	Reaction temperature (°C)	Product distribution (%)[a]						TOF[b] (1/s)	ζ[c]	E_a[d] (kcal/mol)
		Me	Et	Pr	iB	nB	iP			
250	230.5	25.6	—	21.6	52.8	—	—	1.648×10^{-5}	2.30	
	230.5	28.0	—	22.6	49.4	—	—	2.026×10^{-5}	2.39	
	239	32.8	—	30.0	37.2	—	—	5.490×10^{-5}	2.61	
	239	33.2	—	31.7	35.1	—	—	5.549×10^{-5}	2.63	
	248	36.8	3.5	35.9	23.9	—	—	1.607×10^{-4}	2.82	50.0 ± 0.5
	247.5	37.2	3.6	35.5	22.7	1.1	—	1.693×10^{-4}	2.84	(66.3 ± 1.2)
	256	41.6	5.5	36.5	15.7	0.8	—	4.251×10^{-4}	3.03	
	256	41.7	5.5	36.6	15.7	0.5	—	4.407×10^{-5}	3.04	
	246	37.7	3.4	35.0	22.4	1.5	—	1.717×10^{-4}	2.85	
	232	33.5	—	27.3	34.8	4.4	—	4.518×10^{-5}	2.62	
400	215	—	—	—	100.0	—	—	2.863×10^{-6}	1.25	
	215.5	—	—	—	100.0	—	—	2.422×10^{-6}	1.25	
	226	25.0	—	—	75.0	—	—	1.512×10^{-5}	2.19	
	225.5	24.6	—	—	75.4	—	—	1.483×10^{-5}	2.17	
	236	22.9	—	—	77.1	—	—	7.270×10^{-5}	2.11	77.7 ± 3.2
	248	22.6	—	3.9	72.2	0.7	0.7	4.724×10^{-4}	2.12	
	249	23.6	—	4.4	70.9	0.6	0.5	6.421×10^{-4}	2.16	
	232	26.3	—	—	73.7	—	—	4.903×10^{-5}	2.24	
	214.5	47.2	—	—	52.8	—	—	5.248×10^{-6}	3.02	
	248.5	23.2	0.4	4.0	71.2	0.6	0.5	5.844×10^{-4}	2.15	

Note. Footnotes *a–d* as in Table 1.

TABLE 3

Neopentane Conversion over 3 wt% Pd/CaKL: Product Distributions, Reaction Rates, Fragmentation Factors, and Activation Energies

Reduction temperature (°C)	Reaction temperature (°C)	Product distribution (%)[a]						TOF[b] (1/s)	ζ[c]	E_a[d] (kcal/mol)
		Me	Et	Pr	iB	nB	iP			
250	222	—	—	—	100.0	—	—	4.110×10^{-6}	1.25	
	221	39.8	—	—	60.2	—	—	6.129×10^{-6}	2.74	
	231	28.2	—	10.2	61.6	—	—	2.664×10^{-5}	2.35	
	231	27.5	—	11.6	60.9	—	—	2.723×10^{-5}	2.33	
	241.5	29.3	—	18.3	49.6	2.8	—	9.751×10^{-5}	2.43	52.7 ± 0.6
	241	28.9	—	18.0	50.7	2.4	—	9.542×10^{-5}	2.41	(71.2 ± 3.5)
	251	33.6	1.6	25.7	37.9	1.3	—	3.071×10^{-4}	2.64	
	251	33.4	2.0	25.9	37.7	1.1	—	3.190×10^{-4}	2.64	
	237	28.3	—	17.9	50.0	3.8	—	8.015×10^{-5}	2.39	
	222.5	28.9	—	11.2	59.8	—	—	1.696×10^{-5}	2.38	
400	219.5	—	—	—	100.0	—	—	6.019×10^{-6}	1.25	
	220	—	—	—	100.0	—	—	7.303×10^{-6}	1.25	
	231.5	22.1	—	—	73.4	—	4.5	5.314×10^{-5}	2.12	
	230.5	23.4	—	—	72.7	—	4.0	4.966×10^{-5}	2.16	
	239	22.7	—	2.1	73.2	0.1	1.9	1.748×10^{-4}	2.13	81.1 ± 2.0
	238.5	22.5	—	2.2	73.5	—	1.9	1.626×10^{-4}	2.12	
	247.5	23.3	0.6	4.2	70.5	0.8	0.6	5.759×10^{-4}	2.15	
	247	23.3	0.5	4.0	70.8	0.9	0.6	5.463×10^{-4}	2.15	
	235	23.1	—	—	74.0	—	2.9	1.058×10^{-4}	2.14	
	224	24.7	—	—	75.3	—	—	1.875×10^{-5}	2.18	

Note. Footnotes *a–d* as in Table 1.

comparable activity and selectivity, independent of the charge-compensating ion in the zeolite. For all catalysts, the samples reduced at 400°C are more active than those reduced at 250°C. Moreover, the activity of the former samples is stable upon returning from higher to lower temperature, but the latter samples become more active during reaction at high temperature.

The product distribution in Tables 1–3 shows that the samples reduced at 400°C catalyze mainly single C–C fission with CH_4 and iso-C_4H_{10} as major products and a fragmentation factor ζ close to 2, as is typical for Pd. For the sample reduced at 250°C, more CH_4 is formed besides C_3H_8, indicating deeper hydrogenolysis; the fragmentation factor, $\zeta \gg 2.0$; sometimes even

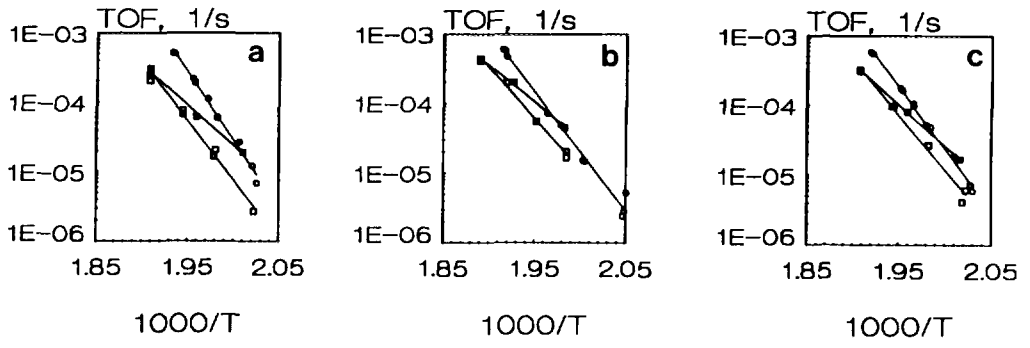

FIG. 1. Arrhenius plots for Pd/L samples reduced at 250°C (squares) and 400°C (circles). Open symbols represent experimental "upwards" points, whereas filled symbols show "downwards" points (for explanation, see text): (a) Pd/LiKL, (b) Pd/KL, and (c) Pd/CaKL.

ethane is detected. Values of $\zeta < 2$ may be erroneous and caused by g.c. underestimation of methane, especially at very low conversion.

b. Temperature Programmed Decomposition

Figures 2, 3, and 4 show TPD spectra for different mass numbers of interest for samples Pd/KL (400), Pd/KL (250), and Pd/KL (250, R), respectively. The area under the curve can be used to calculate relative amounts of that species evolved from the different samples. Table 4 shows the relative amounts of different mass numbers of interest which are evolved during the TPD of ammonia in the three samples. Most of the ammonia present in the sample decomposes into nitrogen and hydrogen. Differences in the amount of nitrogen evolved thus indicate relative differences in the amount of ammonia present in the samples.

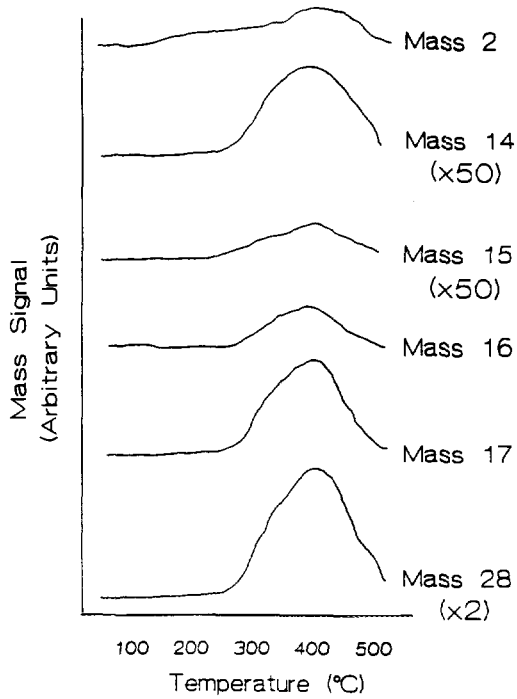

FIG. 3. TPD-MS spectra for Pd/KL (250).

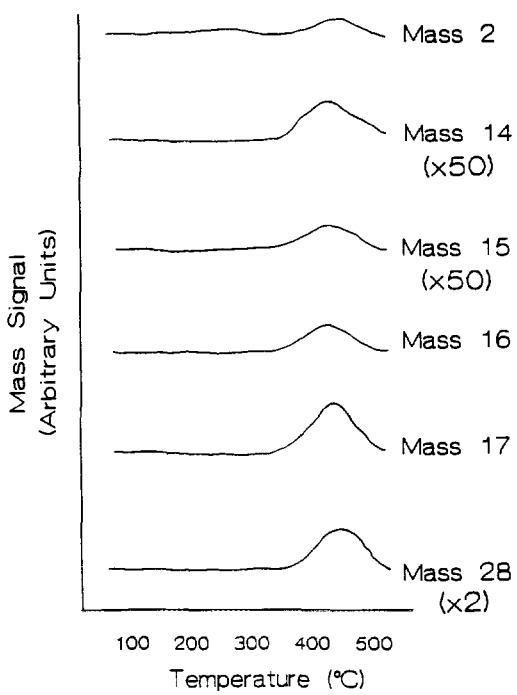

FIG. 2. TPD-MS spectra for Pd/KL (400).

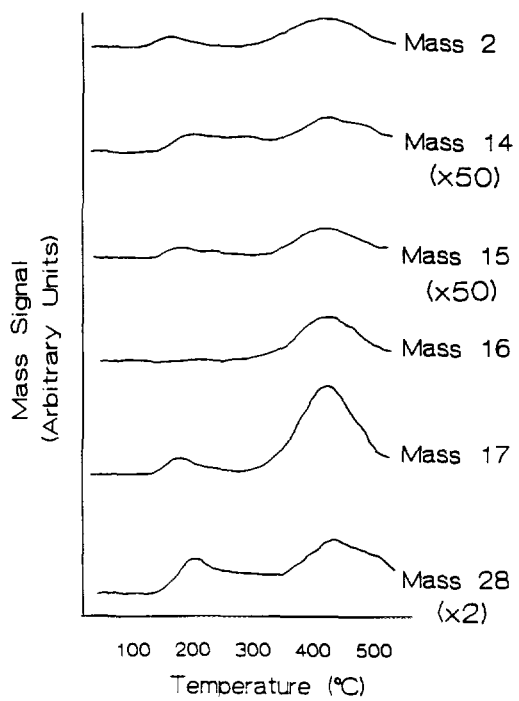

FIG. 4. TPD-MS spectra for Pd/KL (250) after use as a catalyst for 2 h.

TABLE 4

Relative Amounts of Mass Numbers 14, 15, 16, 17, and 28 (Obtained by Integration of TPD-MS Spectra), for Pd/KL (400), Pd/KL (250), and Pd/KL (250, R)

Mass no.	Species	Pd/KL (400)	Pd/KL (250)	Pd/KL (250, R)
2	H_2	1	1.4	0.8
14	N	1	3.1	2.0
15	NH	1	2.9	2.2
16	NH_2	1	2.3	2.1
17	NH_3	1	2.5	2.4
28	N_2	1	4.5	2.7

IV. DISCUSSION

The following findings are discussed: (1) The reduction temperature has a strong effect on the kinetic parameters; (2) the nature of the charge-compensating ion inside the zeolite has only a moderate effect on the catalytic activity; (3) the apparent activation energy for Pd/NaHY is smaller, but that of Pd/XL is much higher than that observed for Pd/SiO_2.

(1)

Turnover frequencies of Pd/L samples that were reduced at 250°C are initially lower than those of samples reduced at 400°C, but the former values increase irreversibly as the reaction temperature is increased, whereas the latter values are stable. These observations are ascribed to incomplete destruction at 250°C of the NH_3 groups which are brought into the zeolite as ligands of Pd^{2+} ions. The TPD data confirm this interpretation; N_2 and H_2 are formed by decomposition of NH_3 and NH_4^+ ions; the TPD peak is located between 350 and 500°C. It follows that at 400°C, when the decomposition rate has its maximum value, most NH_3 ligands and NH_4^+ ions will be destroyed, when the temperature is held for 30 min at this value. This is the case for the samples which are reduced at 400°C. However, these NH_3 groups survive in samples that are reduced at 250°C.

In the absence of ammonia, protons are formed as the coproduct of reducing Pd ions with H_2; these protons are known to form adducts with Pd particles. For Pd/Y such adducts have been shown to have enhanced catalytic activity for neopentane conversion. The TPD study provides evidence that in samples that were originally calcined and reduced at 250°C, ammonia is decomposed during neopentane conversion at 255°C. The concomitant formation of protons and palladium proton adducts would explain the observed increase of the catalytic activity during the catalytic reaction.

It is conceivable that the protons of the Pd-proton adducts are directly involved in the catalysis of neopentane conversion as had been proposed by Bai and Sachtler for another hydrocarbon conversion (*12*). To illustrate this point, the adduct is written simply as containing only one proton. Dissociative adsorption of neopentane on such a complex might be visualized as follows:

$$(CH_3)_3\text{—}C\text{—}CH_3 + H^+\text{—}Pd_n \rightarrow CH_4 + (CH_3)_3\text{—}C^+\text{—}Pd_n,$$

which then reacts with H_2 as

$$(CH_3)_3\text{—}C^+\text{—}Pd_n + H_2 \rightarrow (CH_3)_3\text{—}CH + H^+\text{—}Pd_n.$$

Interestingly, methane and isobutane are indeed the major products on the catalyst samples reduced at 400°C, i.e., after destruction of the NH_4 ions. For the catalysts reduced at 250°C, more methane and propane is formed, suggesting a mechanism where $\alpha\gamma$-adsorption of neopentane on Pd takes place, followed by cleavage of two methyl groups as methane, leaving the C_3 skeleton adsorbed on the Pd surface. This might explain the high methane and propane content of the reaction product. However, this selectivity is not observed with Pd/SiO_2, where isomerization and stepwise splitting of terminal methyl groups prevails at low conversion (*13*). Stepwise demethylation is typical for alkane hydrogenolysis

over palladium (*14*), the higher values of the fragmentation factor, ζ, for Pd/L (250) (Tables 1–3) suggest, therefore, secondary cracking of primary products. This could be a consequence of the extended residence time of the primary reaction products in the one-dimensional channels of zeolite L. Single-file diffusion could conceivably become even more difficult if numerous NH_4^+ ions are present in the channels. This would explain why the ζ-values for Pd/L (250) are initially higher than those for Pd/L (400).

(2)

In comparison to the formation of proton adducts, variation of the charge-compensating ion (Li, K, Ca) inside the zeolite has only a moderate effect on the catalytic performance. Besoukhanova and Barthomeuf report that for Pt/L catalysts that were prepared by impregnation (i.e., no proton formation during metal reduction) the FTIR frequency of adsorbed carbon monoxide changes significantly with the nature of the ion (*7*). The present data show that the apparent activation energy shifts from 88 kcal/mol for LiKL via 81 kcal/mol for CaKL to 77.7 kcal/mol for KL. This may be an indication of an "electronic" interaction between Pd cluster and charge-compensating ion, possibly via zeolite oxygen. It is also possible that the heat of physisorption of neopentane depends on the nature of the ions. If an adsorption equilibrium is established and transport phenomena can be disregarded, the apparent activation energy is given by the difference between the true activation energy and the heat of adsorption of the reactant. Physisorption will also affect the transport processes, as shown below.

(3)

It is evident from Fig. 5 and Tables 1–3, that the apparent activation energy for neopentane conversion over supported Pd strongly depends on the nature of the support. For the Pd/NaHY, apparent activation energies of 35–40 kcal/mol are observed, which are lower than the value of 62 kcal/mol for Pd/SiO_2. For Pd/XL, values up to 88 kcal/mol are found. All data were collected with the same reactor; plotting the apparent activation energies versus the logarithm of the measured pre-exponential factor shows that all points are located near a linear "compensation line." The highest and the lowest activation energies correspond to stable, reversible Arrhenius lines, which were measured after virtually complete destruction of NH_4^+ ions.

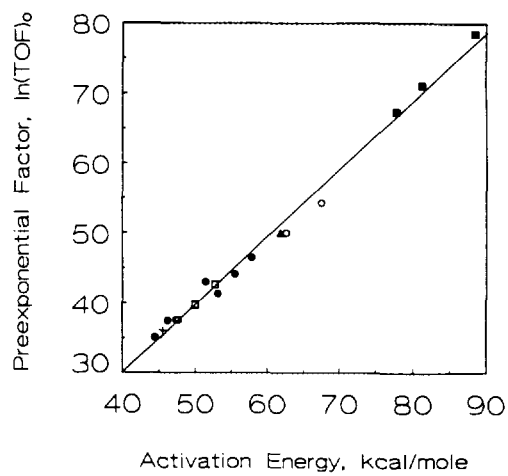

FIG. 5. Compensation effect for neopentane conversion over supported Pd: open squares, Pd/L (250); filled squares, Pd/L (400); filled triangle, Pd/SiO_2 (from (*20*)); filled circles, 2, 4, and 7 wt% Pd/NaY (from (*3*)); open circles, 5 wt% Pd/NaY; and cross, 5.2 wt% Pd/HY (Karpiński, Z., and Sachtler, W. M. H., unpublished).

Such a strong effect of the nature of the zeolite support on the kinetic parameters of a metal catalyzed reaction has, to our knowledge, never been reported before. While the presence of a pre-equilibrium of adsorbed neopentane or some ordinary pore diffusion control might explain lowering of the apparent activation energy for Pd on zeolites vis-à-vis SiO_2, these phenomena fail to explain the high values for L-supported Pd. In view of the indications that the extent of electron-deficiency of the metal might be different on L or Y, one might consider an electronic effect (*7*, *10*,

15); the small changes due to variation of the charge-compensating ion, however, do not lend much support to this hypothesis. It is also not easy to visualize that electronic interaction of a given metal with two silica–aluminates of similar composition but different structure should give rise to large differences in apparent activation energy. While being unable to provide a definitive conclusion on the cause of the unusually large apparent activation energies observed for Pd/XL, we considered, in a purely qualitative way, the possible consequences of the different transport mechanisms in three-dimensional channel systems with "mixing chambers" of Y and the "single-file diffusion" in narrow one-dimensional pores of L.

The free channel apertures (ca. 0.73 nm in L; 0.74 in Y) are quite similar in both zeolites; in the absence of plugging, the neopentane molecule with a kinetic diameter of 0.62 nm (*16*) should be able to diffuse through these pores. In Y diffusion is not a serious problem, as the supercages serve as "mixing chambers" where reactants and products easily mix. Reaction products can therefore easily reach the external surface along one of the numerous paths available from every active site. The situation is different in L. In narrow one-dimensional pores two-way traffic is difficult or impossible; migration of molecules through the channels thus resembles the "string of pearls" situation described by Kärger *et al.* (*9*), i.e., molecules cannot pass each other. A product molecule that has been formed far from the pore mouth is virtually trapped if pores are filled to a high extent with physisorbed reactant molecules. Although the channels in L have bulges, these are not likely to serve as efficient mixing chambers, because their shape is more disc-like in contrast to the virtually spherical supercages in Y. For L-supported Pd at temperatures and pressures where physisorption is significant, analysis of the gas phase thus mainly registers catalytic conversion in the region near the pore mouths. As reaction proceeds, the interior of the channels become occupied with product molecules. Model calculations of the concentration profiles have been published by Kärger *et al.* (*9*). The depth of the region near the channel orifices, where exchange with the gas phase occurs easily, increases with temperature, because physisorption decreases and the rate of single-file diffusion increases. This may result in an increase of the apparent activation energy. Unfortunately we have been unable to find independent literature data supporting this model. In fact, recent results of Larsen and Haller of neopentane conversion over Pt/L zeolites, at partial pressures of the reactants different from ours, did not show such an effect on E_a (*17*). However, in their case catalytic activity reached a steady state only after 2.5 h, whereas no induction period is observed in the present study.

In the case of the Y zeolite, the effect of transport is different; ordinary diffusion takes place which is either so fast that no concentration gradients exist between external and internal regions, or it is less rapid than the chemical reaction and concentration gradients build up. The well-known Wheeler model shows that this type of pore diffusion control lowers the apparent activation energy ultimately to half the true activation energy. It is noteworthy that all E_a values measured in the present work with Pd/Y are lower than that on Pd/SiO_2, but not lower than half that value.

Physisorption of hydrocarbons has been measured for a number of zeolites, including mordenite and L, both with one-dimensional pores. Physisorption is negligible at ~500°C where Pt/KL catalyzed aromatization of hexane is carried out, but appreciable in the 200–300°C region of some catalytic reforming processes and the present study. The isosteric heats of adsorption are generally higher on the Na or K form of the zeolites than on their H form; for instance 21.0 kcal/mol for *n*-hexane on Na–Mor, but 15.7 kcal/mol on H–Mor (*18*). Adsorption of neopentane on L zeolites has been re-

ported by Barrer and Lee (*19*): at 210°C (the highest temperature used by these authors), saturation with neopentane corresponds to 4 cm^3STP/g or roughly 0.5 molecules per unit cell (1 molecule per 1.5 nm pore length). From the graph in that paper, it appears that adsorption is roughly half of saturation at $p_{neopentane}$ = 40 Torr, i.e., 1 molecule per 3 nm pore length. With a zeolite particle size near 1 μm and channels of the same length, this means that 330 molecules are present in each channel. If molecular traffic control does not permit molecules to pass each other inside such a narrow channel, a product molecule which is formed deep in the pore has little chance of escaping to the gas phase.

The concept that geometric factors are, at least partly, responsible for the difference in measured kinetic parameters of L- and Y-supported Pd, does not exclude that additional effects, including electronic interactions, might also play a role.

V. CONCLUSIONS

Coexistence of Pd clusters with zeolite protons results in the formation of Pd proton adducts which display enhanced activity of neopentane conversion. Calcination/reduction at 250°C leaves a high fraction of the NH_3 ligands of the Pd tetraammino-complexes intact; after reduction, these NH_3 molecules neutralize the protons that are generated in the reduction process. Such catalysts are less active than those reduced at a higher temperature (400°C) because the high-temperature pretreatment is essential for ammonia removal. Changes in selectivity (deepness of hydrogenolysis) and apparent activation energy with the pretreatment are compatible with this model.

Variation of the charge-compensating ion X (Li^+, K^+ or Ca^{2+}) in zeolite L has only a small effect on the catalytic properties of Pd/XHL, suggesting that "electronic" effects are not dominant.

Plugging of the narrow one-dimensional channels in L with physisorbed neopentane might explain why more secondary reaction products are observed for Pd/L than for Pd/SiO_2. It is speculated that such plugging might also be a cause for the high E_a observed with Pd/L catalysts.

ACKNOWLEDGMENTS

Financial support by the National Science Foundation, Contract CTS-8911184/02, is gratefully acknowledged. We thank Mr. Brian T. Carvill for elucidating discussions and helping to edit the paper.

REFERENCES

1. Dalla Betta, R. A., and Boudart, M., *in* "Proceedings, 5th International Congress on Catalysis, Miami Beach, 1972 (J. W. Hightower, Ed.), Vol. 2, p. 1329. North-Holland, Amsterdam, 1973.
2. Foger, K., and Anderson, J. R., *J. Catal.* **54,** 318 (1978).
3. Homeyer, S. T., Karpiński, Z., and Sachtler, W. M. H., *Recl. Trav. Chim. Pays-Bas* **109,** 81 (1990).
4. Homeyer, S. T., Karpiński, Z., and Sachtler, W. M. H., *J. Catal.* **123,** 60 (1990).
5. Karpiński, Z., Homeyer, S. T., and Sachtler, W. M. H., *in* "Structure–Activity and Selectivity Relationships in Heterogeneous Catalysis" (R. K. Grasselli and A. W. Sleight, Eds.), p. 203. Studies in Surface Science and Catalysis, Elsevier, Amsterdam, 1991.
6. Stakheev, A. Yu., and Sachtler, W. M. H., *Catal. Today* **12,** 28 (1992).
7. Besoukhanova, C., Guidot, J., Barthomeuf, D., Breysse, M., and Bernard, J. R., *J. Chem. Soc. Faraday Trans. 1* **77,** 1595 (1981).
8. Rieckert, L., *Z. Phys. Chem. N.F.* **43,** 129 (1964).
9. Kärger, J., Petzold, M., Pfeifer, H., Ernst, S., and Weitkamp, J., *J. Catal.* **136,** 283 (1992).
10. Larsen, G., and Haller, G. L., *Catal. Lett.* **3,** 103 (1989).
11. Paál, Z., and Tétényi, P., *Nature* **267,** 234 (1977).
12. Bai, X. L., and Sachtler, W. M. H., *J. Catal.* **129,** 121 (1991).
13. Juszczyk, W., and Karpiński, Z., *J. Catal.* **117,** 519 (1989).
14. Karpiński, Z., *Adv. Catal.* **37,** 45 (1990).
15. Pitchon, V., Guenin, M., and Praliaud, H., *Appl. Catal.* **63,** 333 (1990).
16. Breck, D. W., "Zeolite Molecular Sieves: Structure, Chemistry, and Use," p. 636. Wiley, New York, 1974.
17. Larsen, G., and Haller, G. L., *Catal. Today* **15,** 431 (1992).
18. Eberle, P. E., Jr., *J. Phys. Chem.* **67,** 2404 (1963).
19. Barrer, R. M., and Lee, J. A., *Surf. Sci.* **12,** 341 (1968).
20. Karpiński, Z., Butt, J. B., and Sachtler, W. M. H., *J. Catal.* **119,** 521 (1989).